

# Measuring the impact of flooding on Amazonian trees: photosynthetic response models for ten species flooded by hydroelectric dams

U. M. dos Santos Junior ·  
J. F. de Carvalho Gonçalves ·  
Philip Martin Fearnside

Received: 24 January 2012/Revised: 31 August 2012/Accepted: 26 September 2012/Published online: 13 October 2012  
© Springer-Verlag Berlin Heidelberg 2012

**Abstract** Increasing areas of Amazonian forest are coming under flood stress due to dam construction and greater variability in river flood levels due to climate change. The physiological responses of Amazonian trees subjected to flooding are important to understand the consequences of these changes. Irradiance response curves for photosynthesis obtained from ten tropical tree species growing in flooded areas were used to fit three empirical models. The study was done in floodplains along the Uatumã River, both upstream and downstream of the Balbina Hydroelectric Dam in Brazil's state of Amazonas (01°55'S; 59°28'W). Ten species were studied. Models compared were: non-rectangular hyperbola, rectangular hyperbola, and exponential. All models were quantitatively adequate for fitting the response of measured data on photosynthesis to irradiance for all ten species in the non-flooding and flooding periods. Considerable variation was found among the model estimates of maximum photosynthesis ( $P_{nmax}$ ), dark respiration ( $R_d$ ) and apparent quantum yield of photosynthesis ( $\alpha$ ). For photosynthesis, the two hyperbolas overestimated  $P_{nmax}$  while EXP presented more realistic values. For estimating  $R_d$ , RH presented the most realistic values. To avoid unrealistic value estimates of  $R_d$ , we

recommend adding measured  $R_d$  values to the regressions. The results suggest that the EXP model presented the most realistic  $P_{nmax}$  and  $\alpha$  values, and, in spite of less accuracy in fitting photosynthetic irradiance curves than the RH model, it can be recommended for accessing the information used in photosynthetic irradiance curves for the leaves of tropical trees growing in Amazonian floodplains or in areas that are artificially flooded by dams.

**Keywords** Apparent quantum yield · Carbon · Convexity term · Dark respiration · Global warming · Photosynthesis

## Introduction

The carbon balance of Amazonian forests is a matter of global concern because any significant shift toward gain or loss would translate into climatically significant amounts of atmospheric carbon dioxide (Ometto et al. 2005). Forests gain or lose carbon as a result of a balance between rates of tree growth and recruitment on one side and mortality on the other. These rates are affected by the different stresses to which trees are subjected, such as lack of water, light, or nutrients. One underappreciated stress in the context of Amazonian forests is that of flooding (Costa et al. 2009). The increased variability in river flow levels expected to result from projected climate changes indicates future increases in areas subject to flooding. The record-breaking Amazon floods of 2009, which even submerged part of downtown Manaus, offer a harbinger of this (Nobre and Borma 2009). Massive plans for dam building would subject additional forest areas to flood stress: Brazil's 2011–2020 electrical expansion plan (Brazil, MME 2011) calls for building 30 dams in the country's Amazon region by 2020, or one dam every four months. The physiological

Communicated by E. Priesack.

U. M. dos Santos Junior · J. F. de Carvalho Gonçalves (✉)  
National Institute for Research in the Amazon (MCTI-INPA),  
Laboratory of Plant Physiology and Biochemistry,  
Manaus, Amazonas, Brazil  
e-mail: jfc@inpa.gov.br

P. M. Fearnside  
National Institute for Research in the Amazon (MCTI-INPA),  
Department of Ecology, Manaus, Amazonas, Brazil  
e-mail: pmfearn@inpa.gov.br

responses of Amazonian trees to stress from flooding are therefore important to understanding the consequences of these changes.

Tropical forests play an important role in regional and global CO<sub>2</sub> fluxes and could contribute up to 50 % of total global primary productivity (Grace et al. 2001). Soil fertility differences are believed to explain a gradient of increasing net production from east to west in Amazonia (Malhi et al. 2006). Mature Amazonian forests can act either as sinks or sources, depending on climatic conditions, with droughts such as those during El Niño events resulting in net releases of carbon (Tian et al. 1998, 2000; Saleska et al. 2003; Rice et al. 2004; Davidson et al. 2012). Major Amazonian droughts in 2005 and 2010 caused by warm water in the Atlantic Ocean (rather than El Niño, which is triggered by warm water in the Pacific) dramatically stunted tree growth in the region (Phillips et al. 2009; Lewis et al. 2011). Both of these forms of drought are expected to increase in frequency and severity as a result of global warming (Cox et al. 2004, 2008). On the other hand, a major Amazonian flood occurred during a La Niña event in 2009 that caused excess rainfall in the north and northeast of Amazon region (Marengo et al. 2011). Although the effect of drought dominates interannual variation in production in Amazonia as a whole, the effect of flooding is also an important factor in forest productivity.

Stress from flooding may play a substantial role in limiting the productivity of Amazonian forest trees. Current estimates indicate a large area of Amazonia that is subject to annual flooding. Traditionally, the annually flooded area in the Brazilian portion of the Amazon has been considered to be 70,000 km<sup>2</sup>, or 2 % of Brazil's share of the forest (Goulding 1980). Recently, synthetic-aperture radar (SAR) imagery from the Japanese Earth Resources Satellite (JERS), which can “see” through both clouds and tree cover to detect standing water on the forest floor, has produced much higher estimates, approximately 850,000 km<sup>2</sup> of forest (i.e., not counting savanna wetlands) being subject to flooding throughout the lowland Amazon in all of the countries that share the basin (Melack et al. 2004). This represents 17 % of the forest, or an area more than double that of the US state of California. The areas affected by this “natural” flooding may increase as a result of hydrological impacts from land-use change (Costa et al. 2003) and climate change (Marengo et al. 2009).

Trees undergoing flooding stress are believed to halt or greatly reduce their rates of photosynthesis. At two forest sites located approximately 80 km North of Manaus and 100 km from the Balbina Dam, the Large-Scale Biosphere–Atmosphere (LBA) Project has measured CO<sub>2</sub> fluxes above the forest canopy from two 55-m high towers. Significantly lower carbon uptake at one of the two sites was ascribed to the larger area of seasonally flooded *baixio*

(valley bottom) in the area surrounding the tower (Araújo et al. 2002).

The effect of “natural” flooding is now being joined by the effects of hydroelectric dams. Reservoirs fluctuate in water level, and at their peak water levels they temporally flood surrounding forest. Forests that are flooded permanently or for long periods of the year are killed, but those at slightly higher elevations that are only occasionally flooded for short periods will experience stress, killing some trees and slowing the growth of others. The raising of the water table in the forest surrounding the shoreline stresses trees even when pooled water at the surface is not present. For example, in the forest adjacent to the Samuel Reservoir in the state of Rondônia, in southwestern Amazonia, red dots visible on Landsat satellite imagery indicate this stressed forest (see Fearnside 2005). The Balbina Dam, where the current study was done, has several thousand km of shoreline, including the perimeters of approximately 3,000 islands (e.g., Fearnside 1989). The forested portion of Brazilian Amazonia now has four “large” dams (Curuá-Una, Tucuruí, Balbina and Samuel) and three under construction (Belo Monte, Santo Antônio and Jirau). The only publically available long-range plan, independent of projected construction dates, indicates a total of 79 dams flooding 100,000 km<sup>2</sup> in Brazilian Amazonia (Brazil ELETROBRÁS 1987; Fearnside 1995). The scale of these plans means that better tools are needed to assess dam impacts, including the impact of flooding stress on trees. Quantitative information on the effect of flooding on photosynthesis of tree species in these areas has been lacking and is supplied in the present paper for ten species. Identification of the best models for representing these impacts will facilitate future extension of the knowledge base relating flood stress to photosynthesis in tropical forest trees.

Several studies have been done to quantify the assimilation and emission of CO<sub>2</sub> by different forest types and by the different species that compose the forest ecosystems (Zhan et al. 2003; Oren et al. 2006; Stoy et al. 2006; Mercado et al. 2006). Models of photosynthesis play key roles in estimating primary production of vegetation under different conditions and have been used in ecosystem simulations and ecosystem modeling (Gao et al. 2004; Muraoka and Koizumi 2005). Complex mechanistic models of photosynthesis, such as the biochemical models of Farquhar et al. (1980) for C<sub>3</sub> leaves, have often been applied in studies of photosynthesis mechanisms (Peri et al. 2005). These models are usually derived from known quantitative relationships between different kinds of molecules involved in the biochemical processes of photosynthesis and require rather extensive calibration as well as complex parameterization (Cannell and Thornley 1998). Including a detailed representation of biochemical

processes in the biochemical models is not always advantageous, as compared to the simpler leaf-photosynthetic models (Gao et al. 2004).

Due to the complexity of mechanistic models, empirical models have been used to obtain information from irradiance response curves of photosynthesis under different conditions (Sullivan et al. 1996; Eschenbach et al. 1998; Mielke et al. 2003; Morais 2003; Mielke and Schaffer 2010; Silva et al. 2011). Different models have been observed to produce large differences in estimates of important parameters obtained from photosynthesis-irradiance curves, such as maximum photosynthesis ( $P_{nmax}$ ), dark respiration ( $R_d$ ), and the apparent quantum yield of photosynthesis ( $\alpha$ ). These differences can cause errors in the interpretation of the data.

In spite of the differences among the models used in the literature, little attention has been paid to comparison of characteristics and behavior among models for estimating the main photosynthetic parameters. The goal of this study was to investigate the differences in estimates of the main photosynthetic parameters ( $P_{nmax}$ ,  $R_d$  and  $\alpha$ ) produced by the three traditional models (non-rectangular hyperbola, rectangular hyperbola and exponential) and to analyze the three models by fitting measured data on photosynthesis in ten tropical tree species under flooding and non-flooding conditions.

## Materials and methods

### Study area and species selection

The study was conducted in floodplains along the Uatumã River, both upstream and downstream of the Balbina hydroelectric dam, located about 220 km from Manaus in Presidente Figueiredo County, Amazonas state, Brazil (01°55'S; 59°28'W). The climate at this site is Amw under the Köppen classification system. In the period of the experiment (2005–2007), the annual average rainfall was 2392 mm and average values of minimum and maximum temperature were 23.3 and 33.9 °C, respectively. Monthly rainfall at the study location was obtained from Manaus Energia, the power company that operates the Balbina Dam. The physiological data were collected in two different periods (flooding and non-flooding). The non-flooding period was characterized by the reservoir water level varying between 47.64 and 48.21 m above mean sea level (January and February of 2006 and 2007), and the flooding period was characterized by the water level varying between 50.41 and 50.69 m (June and July of 2006 and 2007). The measurements of light curves were performed on ten plants for each of seven species tolerant to flooding and for three non-tolerant species. After selection of the species in the field, fertile

botanical material was collected for identification in the herbarium of the Instituto Nacional de Pesquisas da Amazônia (INPA). The flood-tolerant species were *Nectandra amazonum* Nees (Lauraceae), *Macrobium angustifolium* (Benth.) Cowan (Caesalpinaceae), *Alchornea discolor* Klotzch (Euphorbiaceae), and *Brosimum lactescens* (S. Moore) C.C. Berg (Moraceae), *Senna reticulata* Willd. (Caesalpinaceae), *Genipa spruceana* Steyerl. (Rubiaceae), *Parinari excelsa* Sabine (Chrysobalanaceae) and the non-tolerant species were *Cecropia concolor* Willd. (Cecropiaceae), *Vismia guianensis* (Aubl.) Choisy (Clusiaceae), and *Vismia japurensis* Reichardt (Clusiaceae).

### Photosynthetic measurements

Measurements of photosynthesis-irradiance ( $P_n$ -I) curves (or “light curves”) were performed on healthy, completely expanded leaves in ten plants per species (ten species) in each period (flooding and non-flooding) from 7:30 to 16:30 h using a LI-6400 portable photosynthesis system (Li-cor, USA) equipped with an artificial irradiance source (6400-02B Red Blue). The  $P_n$ -I curves were derived using the “light curve” routine in the OPEN 3.4 software modified to accommodate eleven levels of photosynthetic photon flux density (PPFD: 0, 25, 50, 75, 100, 250, 500, 750, 1000, 1500, 2000  $\mu\text{mol quanta m}^{-2} \text{s}^{-1}$ ) in decreasing order. The minimum time allowed for the reading to stabilize at each PPFD level was 120 s, the maximum time for saving each reading was 300 s, and the maximum coefficient of variation (C.V.) was 1 %. The Li-cor 6400 was adjusted to a flow rate of 400  $\mu\text{mol s}^{-1}$ . The concentration of  $\text{CO}_2$  (from a  $\text{CO}_2$  cylinder mixed with atmospheric  $\text{CO}_2$ ) was 380  $\mu\text{mol mol}^{-1}$ , and the concentration of  $\text{H}_2\text{O}$  vapor inside the assimilation chamber was  $21 \pm 3 \text{ mmol mol}^{-1}$ . Block temperature was  $31 \pm 1 \text{ }^\circ\text{C}$ . Before each measurement, the leaves were exposed to 1,000  $\mu\text{mol quanta m}^{-2} \text{s}^{-1}$  for an adaptation period of 5–10 min, after which the measurements of the  $P_n$ -I curves were performed.

### Description of the models

Three empirical models were tested: (1) non-rectangular hyperbola (Marshall and Biscoe 1980), (2) rectangular hyperbola (Thornley 1976), and (3) exponential (Iqbal et al. 1997) (Table 1).

In the models:  $I$  is the irradiance ( $\sim$ PPFD);  $P_n$  is the rate of net photosynthesis ( $\mu\text{mol CO}_2 \text{ m}^{-2} \text{ s}^{-1}$ );  $P_{nmax}$  is the maximum photosynthesis;  $R_d$  is dark respiration ( $\mu\text{mol CO}_2 \text{ m}^{-2} \text{ s}^{-1}$ ) corresponding to the value of  $P_n$  when  $I = 0 \text{ } \mu\text{mol m}^{-2} \text{ s}^{-1}$ ;  $\theta$  is a dimensionless convexity term, and  $\alpha$  is the apparent quantum yield of photosynthesis ( $\text{mol CO}_2 \text{ mol quanta}^{-1}$ ).

**Table 1** Non-linear photosynthesis–irradiance models

Model number	Description	Model
1	Non-rectangular hyperbola (NRH)	$P_n = \{[(\alpha I + P_{nmax} + R_d) - ((\alpha I + P_{nmax} + R_d)^2 - 4\alpha I \theta (P_{nmax} + R_d))^{0.5}] / 2\theta\} - R_d$
2	Rectangular hyperbola (RH)	$P_n = \alpha I (P_{nmax} + R_d) / [\alpha I + (P_{nmax} + R_d)] - R_d$
3	Exponential (EXP)	$P_n = (P_{nmax} + R_d) \{1 - \exp[-\alpha I / (P_{nmax} + R_d)]\} - R_d$

A non-rectangular hyperbola (NRH) was fitted according to Model 1 (Table 1). To avoid correlation between  $\alpha$  and  $\theta$  during curve fitting,  $\alpha$  was first found by least-squares regression of the initial linear portion of curve, including darkness (PPFD between 0 and 100  $\mu\text{mol m}^{-2} \text{s}^{-1}$ ). The result of the Kok-effect in estimates of  $\alpha$  was analyzed in this study. For rectangular hyperbolas and exponential models,  $\alpha$  was estimated with the non-linear curves.

In this study, two situations were analyzed. In the first situation, the estimated parameters were  $R_d$ ,  $P_{nmax}$  and  $\alpha$  or  $\theta$ , depending of the model used. In the second situation, a measured dark respiration ( $R_d$ ) term was added to the model and only  $P_{nmax}$  and  $\alpha$  or  $\theta$  were estimated by the models. The “measured”  $\alpha$  was estimated by linear regression of  $P_n$  on PPFD between 0 and 100  $\mu\text{mol m}^{-2} \text{s}^{-1}$ ; the measured  $R_d$  was considered to be the value of  $\text{CO}_2$  flux when PPFD = 0  $\mu\text{mol m}^{-2} \text{s}^{-1}$ ; and the measured  $P_{nmax}$  was considered to be the mean value of  $P_n$  when PPFD  $\geq$  1500  $\mu\text{mol m}^{-2} \text{s}^{-1}$ .

### Statistical analysis

Every model was fitted to measured data from each of the 200 P–I curves using the Levenberg–Marquardt algorithm in the non-linear least-squares estimation routine in the Statistica for Windows (Version 6.0) software (StatSoft Inc., Tulsa, OK, USA). The initial values for  $P_{nmax}$ ,  $R_d$ ,  $\alpha$ , and  $\theta$  were set at 10  $\mu\text{mol CO}_2 \text{ m}^{-2} \text{s}^{-1}$ , 0.1  $\mu\text{mol CO}_2 \text{ m}^{-2} \text{s}^{-1}$ , 0.01  $\text{mol CO}_2 \text{ mol}^{-1}$  photons, and 0.1, respectively, making them coherent with the predicted values. None of the initial values for  $P_{nmax}$ ,  $R_d$ ,  $\alpha$ , and  $\theta$  were modified.

For each model, the goodness of fit was verified by plotting the modeled curve against the mean of ten measured curves for each species, based on the analysis of residuals, the coefficient of determination ( $r^2$ ), the average of unsigned deviation (*Aud*) and the root mean square of error (*RMSE*). The  $r^2$  value was used to evaluate the amount of variation explained by a regression; this statistic is commonly used to select the best regression. Due to the  $r^2$  giving heavy weight to observations with large magnitudes, an additional loss function was used to verify the best fit: average of unsigned deviation ( $\text{Aud \%} = \Sigma (|(\text{Predicted} - \text{measured})| / \text{measured}) \times 100/n$ ). As an alternative statistic to confirm the

best goodness of fit for the models, the root mean square error (*RMSE*), or  $\sqrt{\Sigma \text{Error}^2/n}$ , was reported.

### Results

Comparison of the fits and of the estimates of  $P_{nmax}$ ,  $R_d$ ,  $\alpha$ , and  $\theta$  produced by the models

All three models were adequate ( $P < 0.013$  for all species in the two periods) and showed high coefficients of determination ( $r^2 > 0.94$ ) for all species in both the non-flooding (NFP) and flooding (FP) periods (Table 2). Comparing the goodness of fit of the models, RH generally had the best fit as shown by the lower values of average unsigned deviation (*Aud* %) and root mean square error (*RMSE*) for all of the species studied (Table 2). NRH produced the worse fit.

The three models showed a random distribution of residuals around the predicted values for all species in both periods (Fig. 1). The RH model presented the lowest values of residuals for all levels of PPFD, as compared to the NRH and EXP models (Fig. 1). In general, the NRH and EXP models presented an underestimation of  $P_n$  at PPFD = 0, 25, 500, 750, and 1000  $\mu\text{mol m}^{-2} \text{s}^{-1}$  and an overestimation of  $P_n$  at PPFD = 50, 75, 100, 250, 1500, and 2000  $\mu\text{mol m}^{-2} \text{s}^{-1}$  (Fig. 1).

In Fig. 2, estimates of maximum net photosynthesis ( $P_{nmax}$ ), predicted dark respiration ( $R_d$ ) and predicted apparent quantum yield of photosynthesis ( $\alpha$ ) as calculated by the models, are plotted against the measured values for 200 plants from ten species and two periods (non-flooding and flooding). The best estimate of  $P_{nmax}$  was presented by the EXP model while the two hyperbolas overestimated the values of  $P_{nmax}$  (Fig. 2a, b; Table 3). NHR exhibited values of predicted  $P_{nmax}$  higher than measured  $P_{nmax}$ , varying, depending on the species, from 33.7 to 80.5 % (NFP) and from 7.3 to 62.4 % (FP). RH presented values of  $P_{nmax}$  that were higher than the measured  $P_{nmax}$  by 11–31.1 % (NFP) and by 5.2–36.9 % (FP) (Table 3). On the other hand, the EXP model presented good estimates of  $P_{nmax}$  for all species, presenting a slight underestimation. In addition, EXP showed the best correlation between measured and predicted values of  $P_{nmax}$ , while NHR showed the worse.

**Table 2** Statistical indices for accessing the quantitative performance of non-rectangular hyperbola (NRH), rectangular hyperbola (RH), and exponential (EXP) models describing the irradiance response of

photosynthesis when dark respiration ( $R_d$ ) was estimated by the models in ten tropical tree species in the non-flooding period (NFP) and flooding period (FP)

Species	Non-rectangular hyperbola						Rectangular hyperbola					
	Non-flooding (NFP)			Flooding (FP)			Non-flooding (NFP)			Flooding (FP)		
	$r^2$	Aud (%)	RMSE	$r^2$	Aud (%)	RMSE	$r^2$	Aud (%)	RMSE	$r^2$	Aud (%)	RMSE
<i>N. amazonum</i>	0.993	27.8	0.496	0.994	22.9	0.450	0.999	5.3	0.166	0.999	5.5	0.175
<i>M. angustifolium</i>	0.990	20.4	0.456	0.992	14.9	0.354	1.000	4.7	0.099	0.998	6.3	0.168
<i>A. discolor</i>	0.990	31.3	0.595	0.990	20.9	0.482	0.999	3.9	0.153	0.999	4.9	0.110
<i>B. lactescens</i>	0.975	28.3	0.605	0.984	21.6	0.440	0.994	9.7	0.300	0.998	4.4	0.136
<i>S. reticulata</i>	0.997	33.7	0.623	0.996	17.8	0.661	0.999	15.4	0.284	1.000	5.5	0.184
<i>G. spruceana</i>	0.995	19.3	0.402	0.994	16.1	0.353	0.999	6.4	0.203	0.998	6.2	0.184
<i>P. excelsa</i>	0.992	19.4	0.377	0.995	12.0	0.268	1.000	3.4	0.075	0.996	9.9	0.241
<i>C. concolor</i>	0.996	26.9	0.541	0.975	17.8	0.211	0.999	8.3	0.249	0.999	4.2	0.051
<i>V. guianensis</i>	0.987	17.1	0.523	0.972	16.1	0.128	0.999	4.4	0.133	0.989	10.2	0.081
<i>V. jاپurensis</i>	0.981	31.4	0.587	0.971	16.7	0.150	0.996	7.8	0.257	0.999	5.3	0.032
Average	0.990	25.6	0.520	0.986	17.7	0.350	0.998	6.9	0.192	0.998	6.2	0.136

Species	Exponential					
	Non-flooding (NFP)			Flooding (FP)		
	$r^2$	Aud (%)	RMSE	$r^2$	Aud (%)	RMSE
<i>N. amazonum</i>	0.997	12.8	0.343	0.997	9.4	0.313
<i>M. angustifolium</i>	0.993	11.4	0.368	0.996	5.9	0.246
<i>A. discolor</i>	0.993	20.9	0.487	0.993	15.5	0.396
<i>B. lactescens</i>	0.977	24.4	0.578	0.988	16.5	0.392
<i>S. reticulata</i>	0.999	5.0	0.246	0.999	4.5	0.270
<i>G. spruceana</i>	0.998	8.8	0.246	0.998	6.9	0.220
<i>P. excelsa</i>	0.996	10.7	0.280	0.998	3.3	0.164
<i>C. concolor</i>	0.999	8.4	0.244	0.982	12.0	0.177
<i>V. guianensis</i>	0.990	10.3	0.456	0.983	8.1	0.099
<i>V. jاپurensis</i>	0.984	24.7	0.545	0.987	9.5	0.100
Average	0.993	13.8	0.379	0.992	9.2	0.238

$r^2$  coefficient of determination, Aud(%) the average of unsigned deviation, RMSE the root mean square of error (RMSE)

For  $R_d$  RH presented a good estimate, with mean overestimates of 5.8 % (NFP) and 9.9 % (FP) for all species (Table 4). On the other hand, NRH and EXP exhibited a clear underestimation of  $R_d$ . In addition, all of the models showed negative values of predicted  $R_d$ , indicating problems for interpretation of these data (Fig. 2c, d).

The  $\alpha$  value estimated by linear regressions with exclusion of points from the Kok-effect region (PPFD < 20  $\mu\text{mol m}^{-2} \text{s}^{-1}$ ) had mean underestimations of 7.6 % (NFP) and 8.9 % (FP) as compared to measured  $\alpha$  (PPFD 0–100  $\mu\text{mol m}^{-2} \text{s}^{-1}$ ) (Table 5). The  $\alpha$  estimated by the RH models was, on average, 43.8 (NFP) and 70.0 % (FP) higher than the measured  $\alpha$ , and for the EXP models, the estimated values of  $\alpha$  underestimated by 1.2 % for the flooding period and overestimated by 13.8 % for the

non-flooding period compared to measured  $\alpha$  values, considering all species (Table 5).

Comparison of the fits and of the estimate  $P_{nmax}$ ,  $\alpha$ , and  $\theta$  by the models when  $R_d$  values from measured data were added to the models

When the measured data on  $R_d$  were added to the models for estimation of  $P_{nmax}$  and  $\alpha$ , the accuracy for all models decreased as compared to the models in which estimated values of  $R_d$  were used, as demonstrated by decreasing  $r^2$  values and increasing RMSE values (compare the values in Tables 2 to 6). However, the models were adequate ( $P < 0.01$  for all species and both periods) in the models in which  $R_d$  values were estimated.

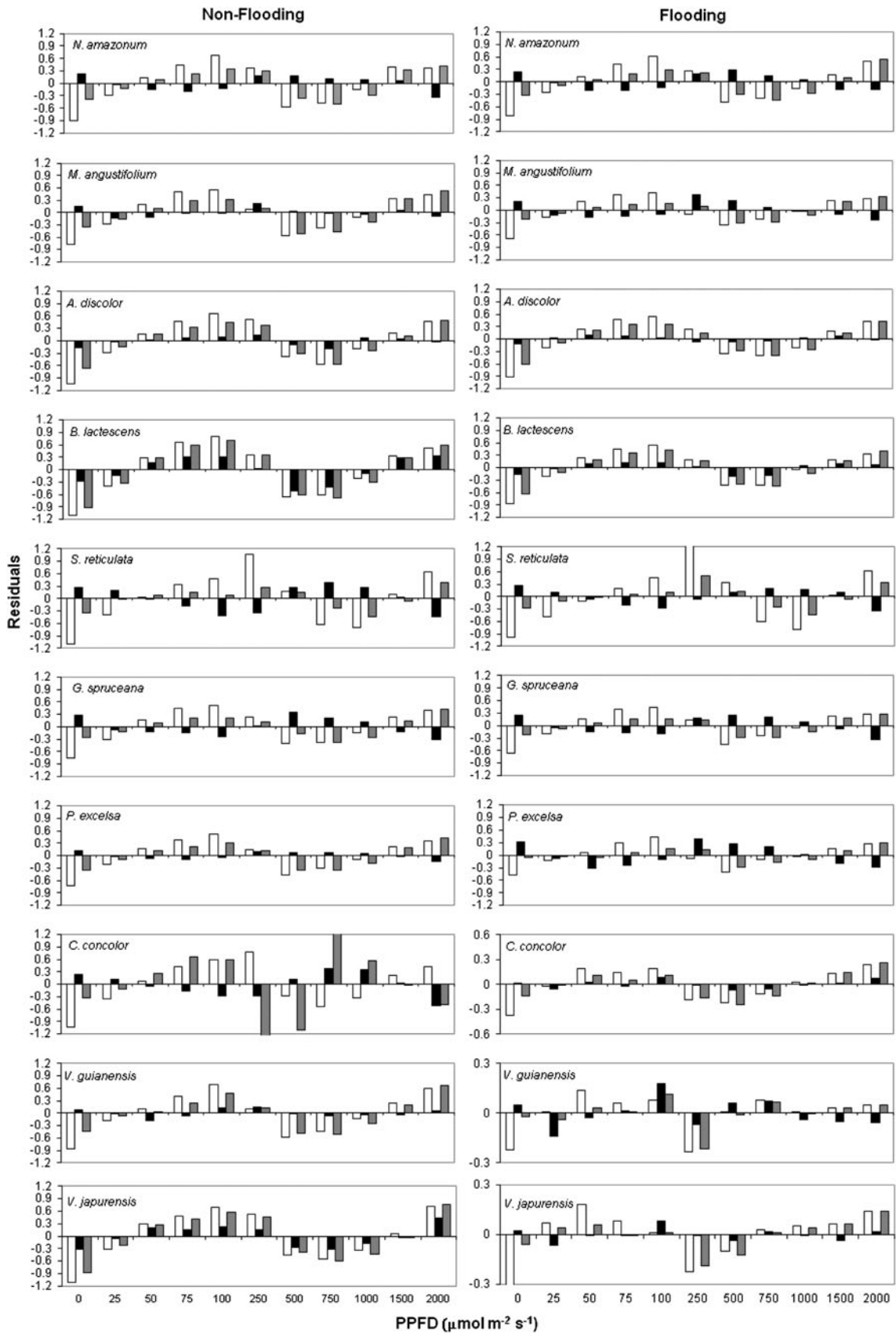


**Fig. 1** Residuals (measured minus predicted values) for net photosynthesis ( $P_n$ ) obtained after adjusting the non-rectangular hyperbola (*white*), the rectangular hyperbola (*black*) and the exponential (*gray*) models to the field data of irradiance curves of photosynthesis, when dark respiration ( $R_d$ ) was estimated by the models, in ten tropical tree species in flooding (*right*) and non-flooding (*left*) periods

The analyses of residuals showed higher values than the residuals from the models in which  $R_d$  was estimated, especially for NRH (Fig. 3). The RH model continued showing the lowest values for residuals for all levels of PPFD (Fig. 3). The distribution of the residuals showed that the NRH and EXP models overestimated  $P_n$  at PPFD =

**Fig. 2** Predicted and measured values of the maximum net photosynthesis ( $P_{nmax}$ , **a, b**), dark respiration ( $R_d$ , **c, d**) estimated by the models and apparent quantum yield ( $\alpha$ , **e, f**) in ten tropical tree species in non-flooding (**a, c, e**) and flooding (**b, d, f**) periods

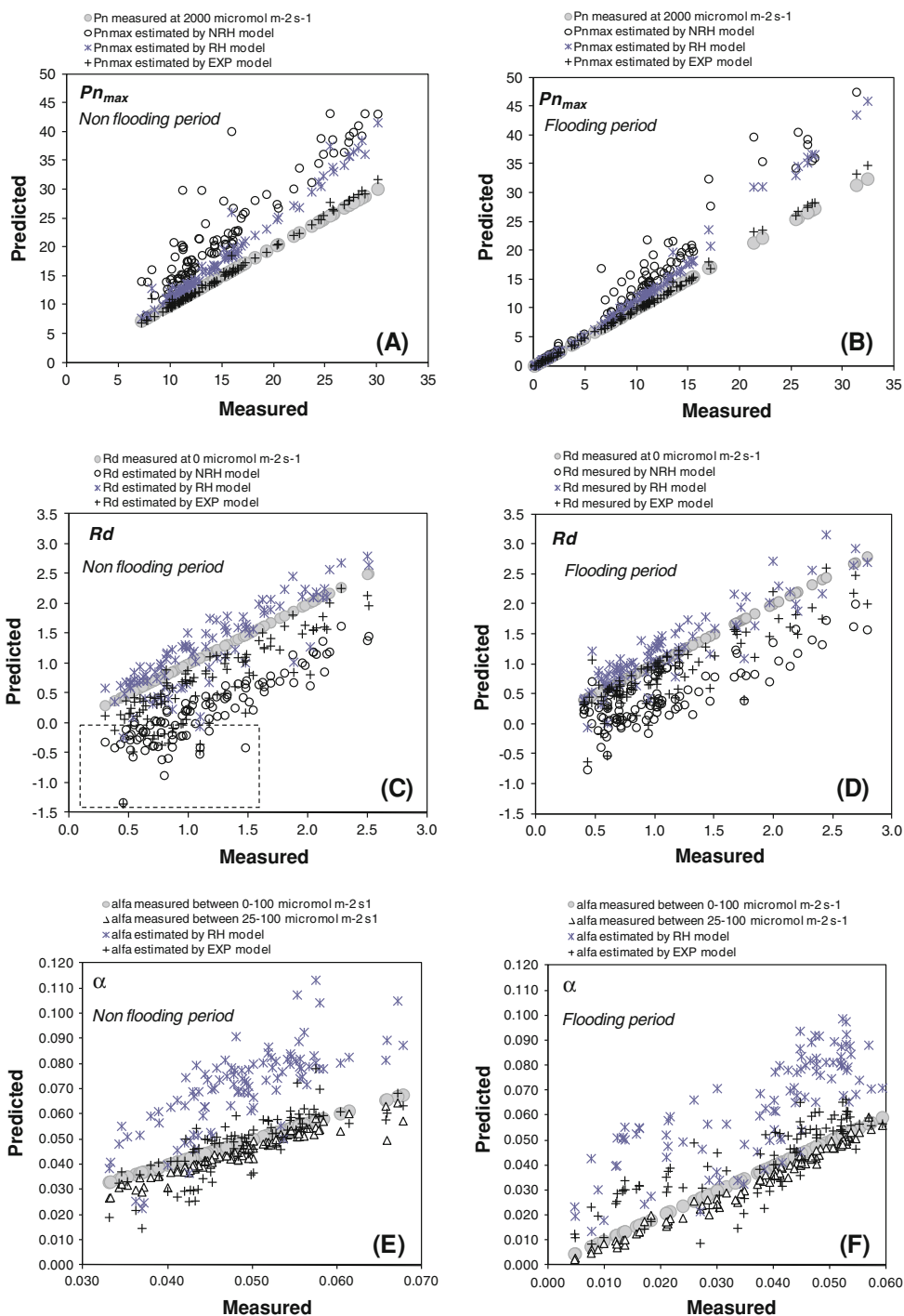


**Table 3** Measured and estimated photosynthesis maxima ( $P_{\text{nmax}}$ ) from three models when dark respiration ( $R_d$ ) was estimated by the models in ten tropical tree species in two flooding periods

Species	Measured		Non-rectangular hyperbola			
			Non-flooding		Flooding	
	Mean (min–max)		%	$r^2$	%	$r^2$
<i>N. amazonum</i>	15.1 (11.6–19.3)	14.2 (11.7–17.1)	38.5	0.888	36.1	0.766
<i>M. angustifolium</i>	11.9 (9.3–15.6)	10.4 (7.5–13.0)	33.7	0.987	29.7	0.508
<i>A. discolor</i>	14.4 (10.1–18.2)	11.6 (6.5–16.9)	70.9	0.473	62.4	0.671
<i>B. lactescens</i>	10.4 (7.2–13.4)	9.2 (5.9–10.9)	80.5	0.414	55.1	0.641
<i>S. reticulata</i>	27.3 (24.8–30.1)	26.6 (21.3–32.4)	43.3	0.754	49.5	0.525
<i>G. spruceana</i>	14.4 (12.0–16.5)	12.0 (10.5–15.3)	34.4	0.982	31.0	0.978
<i>P. excelsa</i>	11.1 (9.6–14.3)	9.6 (7.1–12.9)	37.5	0.889	24.6	0.952
<i>C. concolor</i>	22.8 (17.2–27.7)	3.0 (0.1–9.3)	45.4	0.779	29.5	0.949
<i>V. guianensis</i>	11.6 (7.7–16.1)	1.5 (0.8–2.5)	43.2	0.671	20.7	0.818
<i>V. japurensis</i>	11.1 (7.8–13.1)	2.1 (0.0–4.9)	59.0	0.639	7.3	0.988
All species	15.0 (7.2–30.1)	10.0 (0.0–32.4)	48.3	0.861	41.0	0.958

Species	Rectangular hyperbola				Exponential			
	Non-flooding		Flooding		Non-flooding		Flooding	
	%	$r^2$	%	$r^2$	%	$r^2$	%	$r^2$
<i>N. amazonum</i>	16.4	0.995	16.2	0.998	–2.0	0.996	–1.9	0.994
<i>M. angustifolium</i>	11.9	0.997	12.2	0.996	–3.5	0.998	–2.3	0.995
<i>A. discolor</i>	25.8	0.778	22.4	0.940	1.5	0.920	–0.1	0.982
<i>B. lactescens</i>	11.0	0.971	14.2	0.967	–3.2	0.995	–2.0	0.983
<i>S. reticulata</i>	31.1	0.877	36.9	0.945	3.1	0.974	5.2	0.982
<i>G. spruceana</i>	17.1	0.975	15.3	0.997	–1.5	0.993	–1.6	0.996
<i>P. excelsa</i>	14.0	0.985	13.3	0.992	–2.4	0.994	–2.0	0.990
<i>C. concolor</i>	27.4	0.898	7.6	0.998	1.9	0.970	–6.8	0.998
<i>V. guianensis</i>	16.3	0.861	10.0	0.972	–0.5	0.860	–2.7	0.977
<i>V. japurensis</i>	16.6	0.876	5.2	0.998	–1.4	0.907	–4.9	0.999
All species	20.8	0.980	20.9	0.986	–0.2	0.992	–0.1	0.997

Mean (min–max) of ten repetitions for each species in the non-flooding and flooding periods. The percentages (%) represent changes (positive or negative relative to measured values) that occurred in  $P_{\text{nmax}}$  estimated by the NRH, RH and EXP models

$r^2$  coefficient of determination

25  $\mu\text{mol m}^{-2} \text{s}^{-1}$ , while the models in which  $R_d$  was estimated presented an underestimates (compare Figs. 3 to 1).

In Fig. 4, estimates of maximum net photosynthesis ( $P_{\text{nmax}}$ ) and predicted apparent quantum yield of photosynthesis ( $\alpha$ ) when  $R_d$  was added to the models (as calculated by the models) are plotted against the measured for 200 plants from ten species and two periods (non-flooding and flooding). For the estimated parameters, a better estimation of  $P_{\text{nmax}}$  by NRH was found when  $R_d$  was added, as compared to the situation in which  $R_d$  was estimated by the NRH model (compare values of Tables 7 to 3). For the RH and EXP models, a slight difference was observed, in which the EXP model showed more realistic estimates of  $P_{\text{nmax}}$ , as compared to the two hyperbola models. For  $\alpha$ , RH and EXP models presented better linear correlations

between measured and estimated values of  $\alpha$ , with higher values of  $r^2$  when measured  $R_d$  was included in the models (Table 8). In addition, EXP models presented more realistic estimates of  $\alpha$  as compared to RH models. For  $\theta$  in NRH models, on average, underestimates of 7.0 % (NFP) and 4.5 % (FP) were observed, when measured,  $R_d$  was added to the models, considering all species (Table 9).

## Discussion

### Models fit performance

In this study, all three models were quantitatively adequate ( $P < 0.013$ ) in predicting the behavior of the



**Table 4** Measured and estimated dark respiration ( $R_d$ ) by three models in ten tropical tree species in two flooding periods

Species	Measured		Non-rectangular hyperbola			
			Non-flooding		Flooding	
	Mean (min–max)		%		$r^2$	
<i>N. amazonum</i>	1.44 (0.77–2.51)	1.37 (0.95–2.79)	–62.6	0.916	–60.5	0.955
<i>M. angustifolium</i>	0.61 (0.43–0.88)	0.80 (0.43–1.04)	–128.9	0.412	–85.2	0.829
<i>A. discolor</i>	1.73 (0.86–2.27)	1.84 (1.19–2.69)	–60.2	0.891	–50.2	0.878
<i>B. lactescens</i>	0.74 (0.45–1.17)	0.83 (0.54–1.17)	–150.3	0.328	–104.7	0.655
<i>S. reticulata</i>	1.63 (0.79–2.18)	2.04 (1.32–2.67)	–67.4	0.903	–48.5	0.823
<i>G. spruceana</i>	1.00 (0.59–1.45)	0.78 (0.61–1.06)	–75.2	0.869	–86.5	0.761
<i>P. excelsa</i>	0.56 (0.30–1.03)	0.72 (0.47–1.43)	–130.3	0.759	–67.6	0.252
<i>C. concolor</i>	1.50 (0.99–2.49)	0.97 (0.40–1.69)	–68.6	0.612	–38.4	0.682
<i>V. guianensis</i>	1.08 (0.77–1.48)	0.88 (0.45–1.20)	–77.1	0.488	–25.0	0.963
<i>V. japurensis</i>	1.21 (0.70–2.04)	0.68 (0.40–1.00)	–92.1	0.802	–45.8	0.637
All species	1.15 (0.30–2.51)	1.09 (0.40–2.79)	–81.7	0.770	–58.3	0.692

Species	Rectangular hyperbola				Exponential			
	Non-flooding		Flooding		Non-flooding		Flooding	
	%		$r^2$		%		$r^2$	
<i>N. amazonum</i>	16.2	0.890	18.4	0.893	–27.3	0.852	–23.8	0.872
<i>M. angustifolium</i>	26.1	0.882	25.7	0.780	–56.1	0.240	–26.3	0.783
<i>A. discolor</i>	–9.0	0.680	–6.1	0.815	–37.9	0.777	–32.8	0.794
<i>B. lactescens</i>	–36.5	0.339	–20.5	0.509	–122.3	0.219	–74.8	0.513
<i>S. reticulata</i>	16.9	0.904	12.6	0.540	–21.6	0.880	–13.8	0.613
<i>G. spruceana</i>	29.1	0.969	32.4	0.833	–26.3	0.939	–22.4	0.685
<i>P. excelsa</i>	20.4	0.810	42.8	0.714	–64.7	0.731	–9.0	0.393
<i>C. concolor</i>	15.7	0.601	1.7	0.921	–26.3	0.561	–13.8	0.805
<i>V. guianensis</i>	10.0	0.664	5.5	0.907	–39.1	0.518	–2.6	0.972
<i>V. japurensis</i>	–26.7	0.706	3.4	0.963	–71.6	0.730	–8.7	0.851
All species	5.8	0.749	9.9	0.839	–43.1	0.707	–23.0	0.741

Mean (min–max) of ten repetitions for each species in the non-flooding and flooding periods. The percentages (%) represent changes (positive or negative relative to measured values) that occurred in  $R_d$  estimated by the NRH, RH and EXP models  
 $r^2$  coefficient of determination

photosynthesis-irradiance curves for each species in each period. Similar results were found by Gomes et al. (2006), in which NHR, RH, and EXP models were found to be quantitatively adequate for dwarf coconut. To evaluate the best quantitative performance among the three models, the values of  $r^2$ ,  $Aud$  % and  $RMSE$  were observed. Higher values of  $r^2$  and lower values of  $Aud$  % and  $RMSE$  for RH may indicate better accuracy and quantitative performance compared to the other two models for the majority of the species studied in the two periods, especially for NRH models. Some studies have used the  $F$  test to compare the variability of predictions with the variability of measured data with lower absolute values of  $F$  indicate better quantitative performance (Pachesky et al. 1996; Gomes et al. 2006). Using the  $F$  test, Gomes et al. (2006) concluded that

EXP models had better quantitative performance than the two hyperbolas.

Analyses of residuals confirmed the results shown by the  $Aud$  % and  $RMSE$  values, indicating that RH model presented the better goodness of fit than EXP and NRH models. On the other hand, NHR model showed the highest residuals around the predicted values of  $P_n$ , except for *C. concolor* in the non-flooding period (Fig. 1). For *S. reticulata* (NFP and FP) and *C. concolor* (NFP), the high values of residuals may be the result of the high values of  $P_n$  that these species exhibited. It is interesting to observe that in some PPFd for some species the behavior of residuals for RH was different from the NHR and EXP models. Therefore, while RH models showed an overestimation of residual values, NHR and EXP models showed underestimations

**Table 5** Measured values (including points of Kok-effect region) and estimated apparent quantum yield ( $\alpha$ ) by initial slope excluding points of Kok-effect region, and by the RH and EXP models when dark

respiration ( $R_d$ ) was estimated by the models in ten tropical tree species in two flooding periods

Species	Measured		Estimated excluding Kok-effect					
	Non-flooding		Flooding		Non-flooding		Flooding	
	Mean (min–max)		Mean (min–max)		%	$r^2$	%	$r^2$
<i>N. amazonum</i>	0.054 (0.047–0.061)		0.052 (0.047–0.054)		–6.0	0.952	–6.0	0.916
<i>M. angustifolium</i>	0.048 (0.043–0.053)		0.046 (0.038–0.053)		–6.5	0.918	–8.3	0.988
<i>A. discolor</i>	0.047 (0.036–0.055)		0.041 (0.030–0.052)		–9.6	0.952	–12.0	0.930
<i>B. lactescens</i>	0.043 (0.033–0.054)		0.036 (0.027–0.045)		–9.4	0.974	–12.3	0.926
<i>S. reticulata</i>	0.058 (0.053–0.068)		0.052 (0.045–0.059)		–7.0	0.626	–3.9	0.948
<i>G. spruceana</i>	0.049 (0.043–0.067)		0.044 (0.038–0.048)		–5.3	0.982	–6.7	0.884
<i>P. excelsa</i>	0.041 (0.034–0.052)		0.041 (0.026–0.057)		–7.5	0.989	–4.6	0.975
<i>C. concolor</i>	0.056 (0.047–0.066)		0.020 (0.007–0.041)		–6.6	0.457	–15.6	0.993
<i>V. guianensis</i>	0.049 (0.038–0.057)		0.017 (0.012–0.021)		–7.4	0.902	–13.9	0.781
<i>V. japurensis</i>	0.041 (0.033–0.049)		0.018 (0.005–0.034)		–12.2	0.882	–22.6	0.994
All species	0.049 (0.033–0.068)		0.037 (0.005–0.059)		–7.6	0.923	–8.9	0.986

Species	Rectangular hyperbola				Exponential			
	Non-flooding		Flooding		Non-flooding		Flooding	
	%	$r^2$	%	$r^2$	%	$r^2$	%	$r^2$
<i>N. amazonum</i>	53.8	0.209	57.8	0.166	2.8	0.247	5.9	0.218
<i>M. angustifolium</i>	61.9	0.009	79.5	0.670	6.4	0.001	19.7	0.652
<i>A. discolor</i>	31.6	0.885	37.0	0.773	–9.5	0.862	–9.5	0.735
<i>B. lactescens</i>	24.6	0.034	36.2	0.818	–24.7	0.178	–13.8	0.793
<i>S. reticulata</i>	35.8	0.638	30.4	0.509	2.7	0.451	1.4	0.554
<i>G. spruceana</i>	56.5	0.946	65.1	0.580	6.0	0.952	12.9	0.201
<i>P. excelsa</i>	54.4	0.832	79.4	0.808	1.2	0.786	20.6	0.713
<i>C. concolor</i>	38.2	0.317	117.5	0.774	0.4	0.304	38.7	0.762
<i>V. guianensis</i>	56.5	0.637	184.2	0.013	2.9	0.509	73.5	0.125
<i>V. japurensis</i>	21.7	0.665	147.5	0.753	–15.2	0.567	51.2	0.794
All species	43.8	0.572	70.0	0.607	–1.2	0.647	13.8	0.680

Mean (min–max) of ten repetitions for each species in the non-flooding and flooding periods. The percentages (%) represent changes (positive or negative relative to measured values) that occurred in  $R_d$  estimated by the NRH, RH and EXP models  
 $r^2$  coefficient of determination

of the values of residuals (see *N. amazonum*, *G. spruceana*, Fig. 1).

#### $P_{nmax}$ performance

Estimates of  $P_{nmax}$  varied depending on the model used. The best estimation was presented by the EXP model, while NRH and RH models resulted in large overestimations. A similar result was found by Gomes et al. (2006), who concluded that  $P_{nmax}$  was more realistic when estimated by the EXP model. The good estimation of  $P_{nmax}$  by the EXP model suggests that this empirical model can be used as a submodel for predicting values in productivity models and for environmental modeling of the  $CO_2$  balance.

#### $R_d$ performance—part 1

The most realistic estimation of  $R_d$  was obtained from the RH model, while the EXP and NRH models presented a high underestimates. The underestimation of  $R_d$  can be substantial, as observed in this study for some plants, and the estimated values can be unrealistic (see Fig. 2c, d), with the estimates of  $R_d$  values reaching negative values (for the models,  $R_d$  present positive values). Similar results were found by Vervuren et al. (1999), who observed that  $R_d$  was negative in some cases, suggesting unrealistic estimates of respiratory oxygen production. This fact can be problematic for the interpretation and comprehension of the  $CO_2$  balance in single plants and even more so for vegetation.

**Table 6** Statistical indices for accessing the quantitative performance of non-rectangular hyperbola (NRH), rectangular hyperbola (RH), and exponential (EXP) models describing the irradiance response of

photosynthesis, when measured dark respiration ( $R_d$ ) was added in the models, in ten tropical species in non-flooding (NFP) and flooding period (FP)

Species	Non-rectangular hyperbola						Rectangular hyperbola					
	Non-flooding (NFP)			Flooding (FP)			Non-flooding (NFP)			Flooding (FP)		
	<i>Aud</i> (%)	<i>RMSE</i>	$r^2$	<i>Aud</i> (%)	<i>RMSE</i>	$r^2$	<i>Aud</i> (%)	<i>RMSE</i>	$r^2$	<i>Aud</i> (%)	<i>RMSE</i>	$r^2$
<i>N. amazonum</i>	0.987	40.8	0.705	0.988	35.6	0.641	0.999	12.3	0.189	0.999	12.1	0.202
<i>M. angustifolium</i>	0.981	15.0	0.622	0.984	15.9	0.510	0.999	3.6	0.114	0.998	5.8	0.186
<i>A. discolor</i>	0.977	55.6	0.878	0.976	40.7	0.740	0.999	10.6	0.176	0.999	8.0	0.136
<i>B. lactescens</i>	0.954	23.8	0.824	0.967	27.3	0.641	0.993	5.2	0.315	0.998	5.0	0.149
<i>S. reticulata</i>	0.993	52.5	0.924	0.993	27.2	0.908	0.999	4.3	0.310	1.000	6.9	0.223
<i>G. spruceana</i>	0.990	19.9	0.586	0.988	16.5	0.515	0.998	9.0	0.232	0.998	6.4	0.206
<i>P. excelsa</i>	0.984	15.9	0.545	0.990	13.9	0.377	1.000	2.7	0.087	0.995	9.8	0.267
<i>C. concolor</i>	0.992	41.1	0.837	0.952	34.9	0.293	0.999	3.8	0.264	0.999	4.0	0.051
<i>V. guianensis</i>	0.976	21.7	0.697	0.959	27.2	0.155	0.999	4.6	0.137	0.988	10.3	0.082
<i>V. japurensis</i>	0.962	46.9	0.830	0.944	36.6	0.208	0.996	11.0	0.281	0.999	5.4	0.033
Average	0.979	33.3	0.745	0.974	27.6	0.499	0.998	6.7	0.210	0.997	7.4	0.153

Species	Exponential					
	Non-flooding (NFP)			Flooding (FP)		
	<i>Aud</i> (%)	<i>RMSE</i>	$r^2$	<i>Aud</i> (%)	<i>RMSE</i>	<i>RMSE</i>
<i>N. amazonum</i>	0.996	15.2	0.387	0.996	12.2	0.344
<i>M. angustifolium</i>	0.992	6.2	0.397	0.996	4.6	0.260
<i>A. discolor</i>	0.989	35.6	0.621	0.988	25.7	0.520
<i>B. lactescens</i>	0.968	15.9	0.681	0.982	17.3	0.475
<i>S. reticulata</i>	0.999	21.0	0.310	0.999	7.4	0.309
<i>G. spruceana</i>	0.998	5.8	0.277	0.997	5.3	0.244
<i>P. excelsa</i>	0.994	7.2	0.320	0.998	2.4	0.166
<i>C. concolor</i>	0.999	17.7	0.331	0.980	14.7	0.188
<i>V. guianensis</i>	0.988	9.9	0.491	0.983	7.7	0.099
<i>V. japurensis</i>	0.976	31.1	0.663	0.986	11.0	0.103
Average	0.990	16.5	0.448	0.991	10.8	0.271

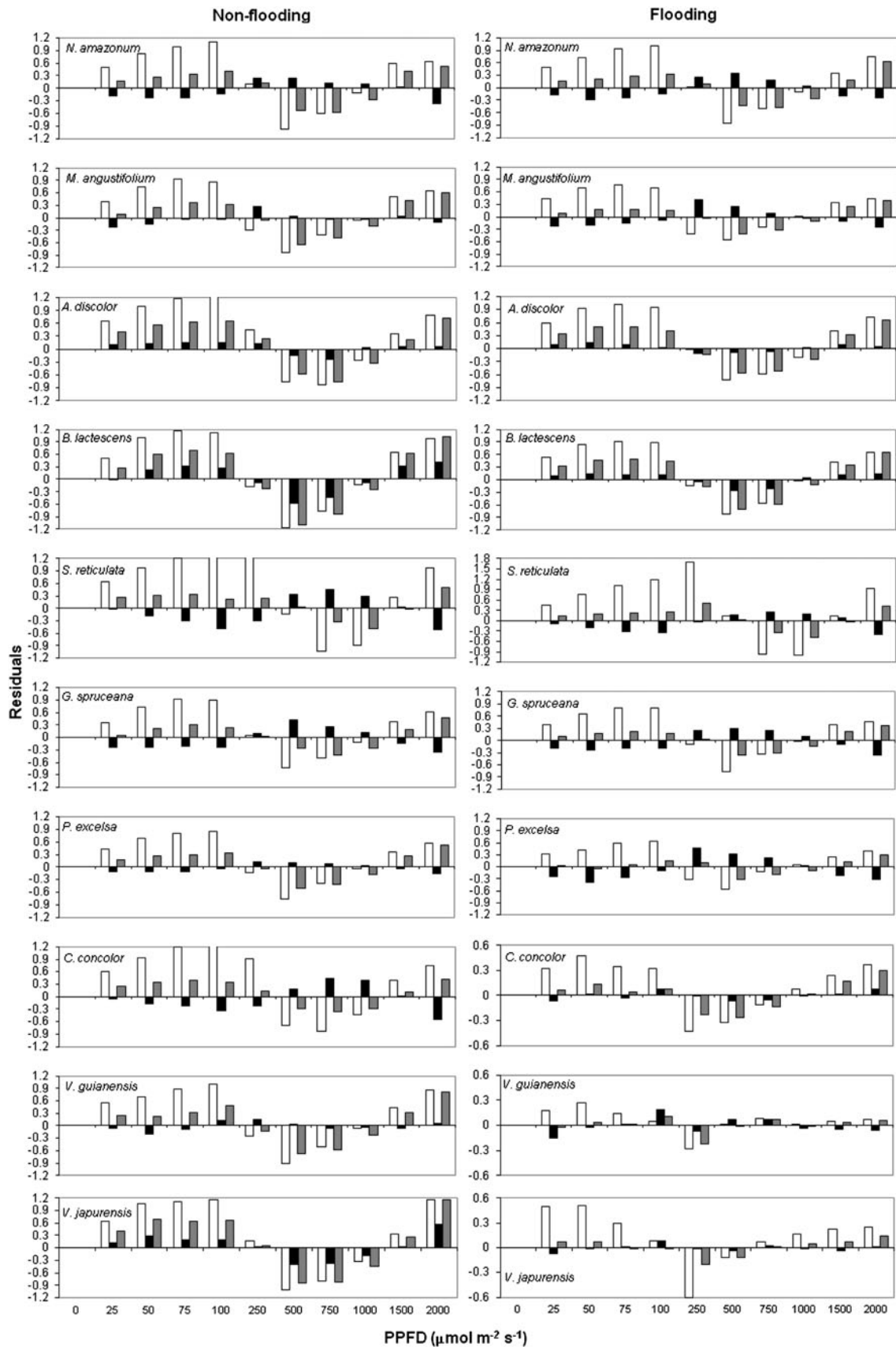
$r^2$  coefficient of determination, *Aud* (%) the average of unsigned deviation, *RMSE* the root mean square of error

$\alpha$  Performance

The calculation of  $\alpha$  varied among the three models tested. First, the Kok-effect region was analyzed in the estimation of  $\alpha$ . The  $\alpha$  value is estimated from the initial slope of the linear regression of the  $P_n$ -I curves, where the net photosynthesis is linear with increasing irradiance. In this study, exclusion of points from the Kok-effect region (Sharp et al. 1984) was found to promote, on average, an underestimation of 7.6 % (NFP) and 8.9 % (FP) of  $\alpha$  as compared to the  $\alpha$  estimated from initial slope including points in the Kok-effect region (e.g., PPFD = 0  $\mu\text{mol m}^{-2} \text{s}^{-1}$ ). Similar results were observed by Clearwater et al. (1999) and Gonçalves and Santos Junior (2005), who found differences of 10 and 12.5 %, respectively. According Leverenz (1987), this difference occurs due to increases in mitochondrial

respiration at very low irradiance (PPFD < 20  $\mu\text{mol m}^{-2} \text{s}^{-1}$ ). The inclusion of the points from the Kok-effect region is responsible for increasing the angular coefficient (slope) of the linear regression from the initial slope and, consequentially, increasing the  $\alpha$  values.

When  $\alpha$  was estimated by the RH model a substantial overestimation was observed as compared to measured  $\alpha$  values (or linearly estimated from PPFD ~0 to 100  $\mu\text{mol m}^{-2} \text{s}^{-1}$ ). This overestimation by RH has been demonstrated in many studies (Mielke et al. 2003; Gomes et al. 2006). In addition, Hootsman and Vermaat (1991) found a satisfactory goodness of fit for the RH model; however, on the basis of the consistent parameter overestimation of  $P_{n\text{max}}$  and  $\alpha$  as observed by Vervuren et al. (1999) and Iwakuma and Yasuno (1983), application of the RH model was considered inappropriate by these authors. For the



◀ **Fig. 3** Residuals for net photosynthesis ( $P_n$ ) values obtained after adjusting the non-rectangular hyperbola (white), the rectangular hyperbola (black) and the exponential (gray) models to field data on irradiance curves of photosynthesis, when measured dark respiration ( $R_d$ ) is included in the models, in ten tropical tree species in flooding and non-flooding periods. \*The residual value for  $P_n$  was 0 at PPFD = 0  $\mu\text{mol m}^{-2} \text{s}^{-1}$  because, in this situation, the estimated  $R_d$  is equal to the  $R_d$  from measured data

EXP model, substantial overestimation of  $\alpha$  was found, on average, for the species in the flooding period, especially for *C. concolor*, *V. guianensis* and *V. japorensis*, that presented low values of  $\alpha$ . These results indicated that the RH and EXP models presented higher overestimation for low values of  $\alpha$ . The linear correlation between  $\alpha$  values estimated by RH and EXP models for all species together was higher ( $r^2 > 0.92$ , data not shown) as compared to the correlation between measured  $\alpha$  values and  $\alpha$  values estimated by the RH model ( $r^2 > 0.57$ ) and the EXP model ( $r^2 > 0.647$ ) (see Table 4), indicating that the principles for calculating  $\alpha$  by RH and EXP models are similar.

Theoretically, the maximum value that  $\alpha$  can reach is  $0.125 \text{ mol mol}^{-1}$ , meaning that 8 mol of photons are required to reduce 1 mol of  $\text{CO}_2$  in the absence of photorespiration (Singsaas et al. 2001). However, due to cyclic photophosphorylation, the maximum  $\alpha$  value may be closer to 0.112 in most  $\text{C}_3$  plants). Comparing the estimating  $\alpha$  by the models, RH model presented values closer to the theoretical maximum  $\alpha$ . However, the  $\alpha$  values estimated by the models were much lower than the theoretical maximum. These results have been found by many researchers in the context of a large set experiments with many different species, with reported values 30–85 % lower than the  $0.125 \text{ mol mol}^{-1}$  theoretical maximum (Clearwater et al. 1999; Marenco et al. 2001a, b; Singsaas et al. 2001; Santos Junior 2003; Gonçalves et al. 2005). The low values of  $\alpha$  may be the result of unfavorable environmental factors (e.g., drought, flooding, high irradiance) and/or may originate from physiological processes that compete with  $\text{CO}_2$  reduction, such as photoinhibition that provokes damage to the photosynthetic apparatus (Groom and Baker 1992; Gonçalves et al. 2005), photorespiration (Sharkey 1988; Peterson 1990; Singsaas et al. 2001), and alternative competitors such as  $\text{NO}_3^-$  and oxygen reduction outside of the photorespiration process (Edwards and Walker 1983; Robinson 1988; Cornic and Briantais 1991).

Thus, for estimates of  $\alpha$ , all models are adequate. However, one must avoid comparing values of  $\alpha$  calculated by different models; in other words, when researchers compare their results to those of others they must pay close attention to how the  $\alpha$  values were estimated.

## $R_d$ performance—part 2

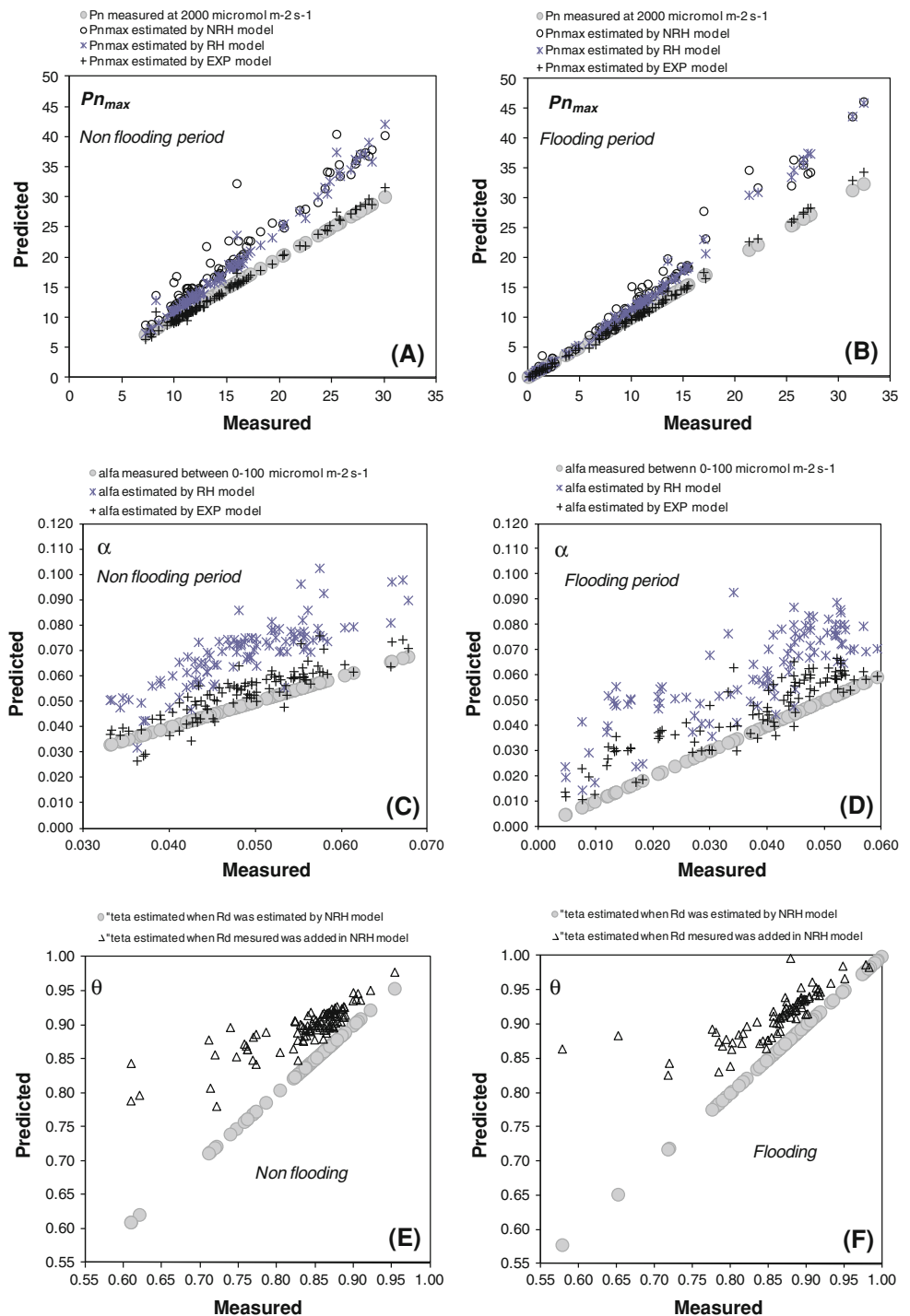
To avoid problems in estimation of  $R_d$  (see discussion above), measured  $R_d$  values were included in the models and only  $P_{n\text{max}}$  and  $\alpha$  or  $\theta$  were estimated by the models. This solution has been used by some researchers to avoid problems with the underestimation of  $R_d$  (Clearwater et al. 1999; Vervuren et al. 1999; Gonçalves et al. 2005). When  $R_d$  was included in the models the regressions, on average, lose accuracy as compared to the situation in which  $R_d$  was estimated, as indicated by the decrease of  $r^2$  values and the increase of *Aud %* (except for RH models in the non-flooding period) and *RMSE*. The loss of accuracy was most evident in the NRH model. This result was confirmed by the analysis of residuals in which the NRH model presented higher values of residuals as compared to the RH and EXP models. This indicates that use of the NRH model may provoke much more error in modeling the photosynthetic irradiance response than the RH and EXP models. In addition, it is clear that, in spite of NRH having been frequently used by many researchers, for the species in this study, it presented the worse quantitative performance, as compared to the RH and EXP models.

For estimation of  $P_{n\text{max}}$ , the EXP models continued presenting the most realistic estimates as compared to the two hyperbolic models, suggesting that the EXP models are most adequate for estimating  $P_{n\text{max}}$  in both situations. EXP also presented better estimates for  $\alpha$  than did the RH models. These results suggest that the main problem presented by the EXP model is in estimating  $R_d$ , because for  $P_{n\text{max}}$  and  $\alpha$ , the EXP model presented the best estimation.

## Convexity term ( $\theta$ ) performance in NRH

For estimating the convexity term ( $\theta$ ), mean values of 0.838 (NFP) and 0.884 (FP) were observed (Table 9). When measured values of  $R_d$  were added to the models, the estimated  $\theta$  increased, on average, by 7.0 and 4.5 % for the non-flooding and flooding periods, respectively. These results were higher than the  $\theta$  values observed by Thomas and Bazzaz (1999) in a study of dipterocarp species ( $\theta$  value ranging from 0.20 to 0.80). On the other hand, Santos Junior (2003) and Gonçalves et al. (2005) found values of  $\theta$  ranging from 0.85 to 0.97 for tree species in Amazonian forest. The low and high values of  $\theta$  are related to gradual and abrupt transitions, respectively, in the light curve, between the region where irradiance is limiting and the region where irradiance is saturated (Thornley 1998). The convexity term has been related to irradiance saturation in chloroplasts, and factors such as irradiance, stress conditions, pigment content, and foliar morphology may affect the  $\theta$  value (Leverenz 1987; Hirose and Werger 1987; Evans 1993; Ogren 1993; Kull and Niinemets 1998).

**Fig. 4** Predicted and measured values of the maximum net photosynthesis ( $P_{nmax}$ , **a, b**), apparent quantum yield ( $\alpha$ , **c, d**) and convexity term ( $\theta$ ) in ten tropical tree species in non-flooding (**a, c, e**) and flooding (**b, d, f**) periods. \*Dark respiration was not estimated by the models because the measured  $R_d$  was added to the models



## Conclusions

In this study, all three models were quantitatively adequate for fitting the response of measured data of photosynthesis to irradiance, in all ten species in the non-flooding and flooding periods. However, RH and EXP were more adequate than NRH in both situations in which  $R_d$  was estimated or in which the measured  $R_d$  was added to the

regression. For parameter estimation, considerable variation was found among estimates of  $P_{nmax}$ ,  $R_d$ , and  $\alpha$  among the models. These differences must be considered in interpreting the data and in making comparisons with the results of other researchers. For photosynthesis, the two hyperbolas overestimate  $P_{nmax}$  while EXP presented more realistic values. Considering the estimation of  $R_d$ , the RH model presented the most realistic values, as compared to

**Table 7** Estimated photosynthesis maxima ( $P_{nmax}$ ) from three models when measured dark respiration ( $R_d$ ) was added to the models in ten tropical tree species in two flooding periods

Species	Non-rectangular hyperbola				Rectangular hyperbola				Exponential			
	Non-flooding		Flooding		Non-flooding		Flooding		Non-flooding		Flooding	
	%	$r^2$	%	$r^2$	%	$r^2$	%	$r^2$	%	$r^2$	%	$r^2$
<i>N. amazonum</i>	22.0	0.962	20.4	0.930	17.2	0.994	17.0	0.998	-2.8	0.993	-2.6	0.983
<i>M. angustifolium</i>	17.0	0.993	13.4	0.869	12.4	0.997	12.5	0.993	-4.2	0.997	-3.1	0.984
<i>A. discolor</i>	42.5	0.622	32.2	0.912	23.1	0.886	21.3	0.951	-1.1	0.960	-2.5	0.985
<i>B. lactescens</i>	26.9	0.915	26.5	0.816	9.1	0.951	12.5	0.983	-7.6	0.954	-5.3	0.990
<i>S. reticulata</i>	32.1	0.805	37.5	0.711	32.3	0.833	38.0	0.968	2.5	0.957	4.5	0.992
<i>G. spruceana</i>	21.1	0.989	17.9	0.992	18.2	0.973	16.3	0.996	-1.9	0.991	-2.2	0.997
<i>P. excelsa</i>	19.7	0.964	12.8	0.967	14.4	0.984	14.3	0.990	-3.3	0.991	-2.2	0.988
<i>C. concolor</i>	32.2	0.814	33.2	0.977	28.3	0.902	7.6	0.997	1.2	0.968	-7.7	0.997
<i>V. guianensis</i>	20.9	0.824	7.4	0.842	16.5	0.852	10.3	0.970	-1.7	0.849	-3.0	0.977
<i>V. japorensis</i>	32.1	0.416	27.8	0.935	12.9	0.967	5.3	0.998	-6.0	0.990	-5.2	0.999
All species	27.7	0.945	34.3	0.972	20.8	0.985	21.2	0.986	-1.6	0.993	-1.1	0.997

See Mean (min–max) of measured  $P_{nmax}$  in Table 3. The percentages (%) represent changes (positive or negative relative to measured values) that occurred in  $P_{nmax}$  estimated by the NRH, RH and EXP models

$r^2$  coefficient of determination

**Table 8** Estimated apparent quantum yield ( $\alpha$ ) from the RH and EXP models when measured dark respiration ( $R_d$ ) was added to the models, in ten tropical tree species in two flooding periods

Species	Rectangular hyperbola				Exponential			
	Non-flooding		Flooding		Non-flooding		Flooding	
	%	$r^2$	%	$r^2$	%	$r^2$	%	$r^2$
<i>N. amazonum</i>	45.6	0.314	47.9	0.256	11.8	0.380	13.8	0.273
<i>M. angustifolium</i>	53.8	0.042	67.1	0.630	16.9	0.055	26.0	0.678
<i>A. discolor</i>	33.5	0.884	42.3	0.706	2.8	0.892	9.4	0.741
<i>B. lactescens</i>	39.7	0.415	45.9	0.793	4.4	0.389	9.6	0.771
<i>S. reticulata</i>	30.7	0.881	25.4	0.696	7.0	0.834	4.6	0.706
<i>G. spruceana</i>	45.5	0.940	53.2	0.591	12.5	0.940	17.4	0.666
<i>P. excelsa</i>	48.4	0.917	61.8	0.903	13.0	0.927	23.6	0.913
<i>C. concolor</i>	33.1	0.578	114.7	0.820	6.3	0.633	53.0	0.907
<i>V. guianensis</i>	52.4	0.848	169.1	0.003	15.8	0.859	77.2	0.109
<i>V. japorensis</i>	37.0	0.828	142.6	0.874	2.3	0.744	59.1	0.928
All species	41.7	0.696	64.7	0.653	9.4	0.773	23.6	0.808

See Mean (min–max) of measured  $\alpha$  in Table 5. The percentages (%) represent changes (positive or negative relative to measured values) that occurred in  $P_{nmax}$  estimated by the RH and EXP models

$r^2$  coefficient of determination

the NRH and EXP models. However, all models presented problems to estimate  $R_d$ , because for any plants the estimated values were biologically impossible to explain. To avoid this situation, especially for the NRH and EXP models, the solution is to add the measured  $R_d$  term to the regression. When the  $R_d$  term was added, EXP presented

the most realistic estimation of  $P_{nmax}$  and  $\alpha$ , as compared to the RH, and NRH models, which continued to overestimate  $P_{nmax}$ . Thus, we conclude that: (a)  $R_d$  should be added to the regressions to avoid problems of unrealistic estimated values of  $R_d$ ; (b) The NRH model, in spite of being frequently used, was less accurate in fitting the photosynthetic

**Table 9** Estimated convexity term ( $\theta$ ) by non-rectangular hyperbola when dark respiration ( $R_d$ ) was estimated by the models, in ten tropical tree species in two flooding periods

Species	Measured		Non-rectangular hyperbola			
	Non-flooding	Flooding	Non-flooding		Flooding	
	Mean (min–max)	Mean (min–max)	%	$r^2$	%	$r^2$
<i>N. amazonum</i>	0.862 (0.824–0.909)	0.869 (0.815–0.897)	5.4	0.783	5.1	0.903
<i>M. angustifolium</i>	0.867 (0.827–0.906)	0.890 (0.719–0.948)	5.9	0.973	5.2	0.960
<i>A. discolor</i>	0.813 (0.713–0.922)	0.816 (0.652–0.897)	7.1	0.947	9.2	0.302
<i>B. lactescens</i>	0.761 (0.610–0.903)	0.792 (0.578–0.893)	15.3	0.717	12.1	0.515
<i>S. reticulata</i>	0.865 (0.839–0.883)	0.860 (0.799–0.901)	3.2	0.720	3.1	0.994
<i>G. spruceana</i>	0.872 (0.856–0.887)	0.881 (0.864–0.918)	4.5	0.660	4.6	0.820
<i>P. excelsa</i>	0.857 (0.831–0.888)	0.904 (0.860–0.992)	6.2	0.897	4.1	0.971
<i>C. concolor</i>	0.858 (0.822–0.889)	0.908 (0.776–0.999)	3.9	0.679	1.5	0.611
<i>V. guianensis</i>	0.858 (0.769–0.954)	0.950 (0.811–0.994)	6.9	0.894	2.9	0.917
<i>V. japorensis</i>	0.767 (0.610–0.852)	0.966 (0.906–0.990)	13.5	0.864	3.3	0.105
All species	0.838 (0.610–0.954)	0.884 (0.578–0.999)	7.0	0.7334	4.5	0.724

Mean (min–max) of ten repetitions for each species in non-flooding and flooding periods. The percentages (%) represent changes (positive or negative relative to measured values) that occurred in  $\theta$  estimated by the NRH model when  $R_d$  was added to the model

$r^2$  coefficient of determination

irradiance curves and performed poorly in estimating  $P_{nmax}$ , as compared to the RH and EXP models; (c) The RH model presented the best accuracy to fitting the photosynthetic irradiance curves and can be recommended for adjusting the light curves. However, the RH models presented problems to overestimated  $P_{nmax}$  and  $\alpha$ ; (d). The EXP model presented most realistic  $P_{nmax}$  and  $\alpha$  values and, in spite of showing less accuracy in fitting photosynthetic irradiance curves than the RH model, this model can be recommended for accessing photosynthetic irradiance curves for the leaves of tropical trees growing in Amazon floodplains or in artificially flooded areas, such as dams. These curves constitute a key tool for understanding the impact of flooding on carbon balance in Amazonian forests that are being increasingly subjected to stress from flooding.

**Acknowledgments** The authors thank the Conselho Nacional de Desenvolvimento Científico e Tecnológico (CNPq); the Fundação de Amparo à Pesquisa do Estado do Amazonas (FAPEAM), the Large-Scale Atmosphere-Biosphere Experiment in Amazonia (LBA), the Instituto Chico Mendes (ICMBio), the Manaus Energia, the IBAMA, and the entire team of the Laboratory of Plant Physiology and Biochemistry. J.F.C Gonçalves and P.M. Fearnside acknowledge fellowships provided by CNPq.

## References

Araújo AC, Nobre AD, Kruijt B, Dallarosa R, Elbers J, Stefani P, Von Randow C, Manzi AO, Gash JHC, Kabat P (2002) Comparative measurements of CO<sub>2</sub> exchange for two towers in an Amazonian rainforest: the LBA Manaus site. *J Geophys Res* 107(D20). doi: [10.1029/2001JD000676](https://doi.org/10.1029/2001JD000676)

- Brazil, ELETROBRÁS (1987) Plano 2010: relatório geral. Plano nacional de energia elétrica 1987/2010 (Dezembro de 1987). Centrais Elétricas do Brasil (ELETROBRÁS), p 269
- Brazil, MME (2011) Plano decenal de expansão de energia 2020, vol 2. MME (Ministério de Minas e Energia), Empresa de Pesquisa Energética, Rio de Janeiro
- Cannell MGR, Thornley JHM (1998) Temperature and CO<sub>2</sub> responses of leaf and canopy photosynthesis: a clarification using the non-rectangular hyperbola model of photosynthesis. *Ann Bot* 82:883–892
- Clearwater MJ, Susilawaty R, Efendi R, Gardingen PR (1999) Rapid photosynthetic acclimation of *Shorea johorensis* seedlings after logging disturbance in Central Kalimantan. *Oecologia* 121:478–488
- Cornic G, Briantais J (1991) Partitioning of photosynthetic electron flow between CO<sub>2</sub> and O<sub>2</sub> reduction in a C<sub>3</sub> leaf (*Phaseolus vulgaris* L.) at different CO<sub>2</sub> concentration and during drought stress. *Planta* 183:178–184
- Costa MH, Botta A, Cardille JA (2003) Effects of large-scale changes in land cover on the discharge of the Tocantins River, southeastern Amazonia. *J Hydrol* 283:206–217
- Costa MH, Coe MT, Guyot JL (2009) Effects of climatic variability and deforestation on surface water regimes. In: Keller M, Bustamante M, Gash J, da Silva Dias P (eds) Amazonia and global change. geophysical monograph series, vol 186. American Geophysical Union (AGU), Washington, DC, pp 543–553
- Cox PM, Betts RA, Collins M, Harris PP, Huntingford C, Jones CD (2004) Amazonian forest dieback under climate-carbon cycle projections for the 21st century. *Theor Appl Climatol* 78:137–156
- Cox PM, Harris PP, Huntingford C, Betts RA, Collins M, Jones CD, Jupp TE, Marengo JA, Nobre CA (2008) Increasing risk of Amazonian drought due to decreasing aerosol pollution. *Nature* 453:212–215
- Davidson EA, Araújo AC, Artaxo P, Balch JK, Brown JF, Bustamante MMC, Coe MT, Defries RS, Keller M, Longo M, Munger JW, Schroeder W, Soares-Filho BS, Souza CM Jr, Wofsy SC (2012) The Amazon basin in transition. *Nature* 481:321–328



- Edwards E, Walker D (1983)  $C_3$ ,  $C_4$ : mechanisms, and cellular and environmental regulation, of photosynthesis. Blackwell, Oxford
- Eschenbach C, Glauner R, Kleine M, Kappen L (1998) Photosynthesis rates of selected tree species in lowland dipterocarp rainforest of Sabah, Malaysia. *Trees* 12:356–365
- Evans JR (1993) Photosynthetic acclimation and nitrogen partitioning within theoretical optimum. *Aust J Plant Physiol* 20:69–82
- Farquhar GD, von Caemmerer S, Berry JA (1980) A biochemical model of the photosynthetic  $CO_2$  assimilation in leaves of  $C_3$  species. *Planta* 149:78–90
- Fearnside PM (1989) Brazil's balbina dam: environment versus the legacy of the pharaohs in Amazonia. *Environ Manag* 13: 401–423
- Fearnside PM (1995) Hydroelectric dams in the Brazilian Amazon as sources of 'greenhouse' gases. *Environ Conserv* 22:7–19
- Fearnside PM (2005) Brazil's Samuel dam: lessons for hydroelectric development policy and the environment in Amazonia. *Environ Manag* 35:1–19
- Gao Q, Zhang X, Huang Y, Xu H (2004) A comparative analyses of four models of photosynthesis for 11 plant species in the Loess Plateau. *Agric For Meteorol* 126:203–222
- Gomes FP, Oliva MA, Mielke MS, Almeida A-AF, Leite HG (2006) Photosynthetic irradiance-response in leaves of dwarf coconut palm (*Cocos nucifera* L. "nana", Araceae): comparison of three models. *Sci Hortic* 109:101–105
- Gonçalves JFC, Santos Junior UM (2005) Assimilação de carbono e indicadores de estresse da Amazônia. In: Nogueira RJMC, Araújo EL, Willadino LG, Cavalcante UMT (eds) Estresses ambientais: danos e benefícios em plantas, Chap 15:165–181. UFRPE, Imprensa Universitária, Recife, p 500. ISBN 85-87459-20-1
- Gonçalves JFC, Barreto DCS, Santos Junior UM, Fernandes AV, Sampaio PTB, Buckeridge MS (2005) Growth, photosynthesis and stress indicators in young rosewood plants (*Aniba rosaeodora* Ducke) under different light intensities. *Braz J Plant Physiol* 17:325–334
- Goulding M (1980) The fishes and the forest: explorations in Amazonian natural history. University of California Press, Berkeley, p 280
- Grace J, Malhi Y, Higuchi N, Meir P (2001) Productivity and carbon fluxes of tropical rain forest. In: Roy HAM (ed) Global terrestrial productivity. Academic Press, San Diego
- Groom QJ, Baker NR (1992) Analysis of light-induced depressions of photosynthesis in leaves of a wheat crop during the winter. *Plant Physiol* 100:1217–1223
- Hirose T, Werger MJA (1987) Nitrogen use efficiency in instantaneous and daily photosynthesis of leaves in canopy of a *Solidago altissima* stand. *Physiol Plant* 70:215–222
- Hootsman MJM, Vermaat JE (1991) Light-response curves of *Potamogeton pectinatus* L. as a function of plant age and irradiance level during growth. In: Macrophytes: a key to understanding changes caused by eutrophication in shallow freshwater ecosystems. Ph.D. Thesis, International Institute for Hydraulic and Environmental Engineering, Delft, pp 57–130
- Iqbal RM, Rao A-R, Rasul E, Wahid A (1997) Mathematical models and response functions in photosynthesis: an exponential model. In: Pessaraki M (ed) Handbook of photosynthesis. Marcel Dekker Inc., New York, pp 803–810
- Iwakuma T, Yasuno M (1983) A comparison of several mathematical equations describing photosynthesis-light curve for natural phytoplankton population. *Arch Hydrobiol* 97:208–226
- Kull O, Niinemets U (1998) Distribution of leaf photosynthetic properties in tree canopies: comparison of species with different shade tolerance. *Funct Ecol* 12:472–479
- Leverenz JW (1987) Chlorophyll content and the light response curve of shade-adapted conifer needles. *Physiol Plant* 71:20–29
- Lewis SL, Brando PM, Phillips OL, van der Heijden GMF, Nepstad D (2011) The 2010 Amazon drought. *Science* 331:554
- Malhi Y, Wood D, Baker TR, Wright J, Phillips OL, Cochrane T, Meir P, Chave J, Almeida S, Arroyo L, Higuchi N, Killeen T, Laurance SG, Laurance WF, Lewis SL, Monteagudo A, Neill DA, Vargas PN, Pitman NCA, Quesada CA, Salomão R, Silva JNM, Lezama AT, Terborgh J, Martínez RV, Vinceti B (2006) The regional variation of aboveground live biomass in old-growth Amazonian forests. *Global Change Biol* 12:1107–1138
- Marengo RA, Gonçalves JFC, Vieira G (2001a) Leaf gas exchange and carbohydrates in tropical trees differing in successional status in two light environments in central Amazonia. *Tree Physiol* 21:1311–1318
- Marengo RA, Gonçalves JFC, Vieira G (2001b) Photosynthesis and leaf nutrient contents in *Ochroma pyramidale* (Bombacaceae). *Photosynthetica* 39:539–543
- Marengo JA, Jones R, Alves LM, Valverde MC (2009) Future change of temperature and precipitation extremes in South America as derived from the PRECIS regional climate modeling system. *Int J Climatol* 30:1–15
- Marengo JA, Tomasella J, Soares WR, Alves LM, Nobre CA (2011) Extreme climatic events in Amazon basin: climatological and hydrological context of recent floods. *Theor Appl Climatol*. doi: 10.1007/s00704-011-0465-1
- Marshall B, Biscoe PV (1980) A model for  $C_3$  leaves describing the dependence of net photosynthesis on irradiance. *J Exp Bot* 31:29–39
- Melack JM, Hess LL, Gastil M, Forsberg BR, Hamilton SK, Lima IBT, Novo EMLM (2004) Regionalization of methane emissions in the Amazon Basin with microwave remote sensing. *Global Change Biol* 10:530–544
- Mercado L, Lloyd J, Carswell F, Malhi Y, Meir P, Nobre AD (2006) Modelling Amazonian forest eddy covariance data: a comparison of big leaf versus sun/shade models for C-14 tower at Manaus I. Canopy photosynthesis. *Acta Amazonica* 36:69–82
- Mielke MS, Schaffer B (2010) Leaf gas exchange, chlorophyll fluorescence and pigment indexes of *Eugenia uniflora* L. in response to changes in light intensity and soil flooding. *Tree Physiol* 30:45–55
- Mielke MS, Almeida A-AF, Gomes FP, Aguiar MAG, Mangabeira PAO (2003) Leaf gas exchange, chlorophyll fluorescence and growth responses of *Genipa americana* seedlings to soil flooding. *Environ Exp Bot* 50:221–231
- Morais RR (2003) Ecofisiologia de espécies arbóreas crescidas sob condições de plantios na Amazônia central. Manaus, INPA/UFAM 158 p
- Muraoka H, Koizumi H (2005) Photosynthetic and structural characteristics of canopy and shrub trees in a cool-temperate deciduous broadleaved forest: implication to ecosystem carbon gain. *Agric For Meteorol* 134:39–59
- Nobre CA, Borma LS (2009) 'Tipping points' for the Amazon forest. *Curr Opin Environ Sustain* 1:28–36. doi:10.1016/j.cosust.2009.07.003
- Ogren E (1993) Convexity of the photosynthetic irradiance-response curve in relation to intensity and direction of irradiance during growth. *Plant Physiol* 101:1013–1019
- Ometto JP, Nobre AD, Rocha H, Artaxo P, Martinelli L (2005) Amazônia and the modern carbon cycle: lessons learned. *Oecologia* 143:483–500
- Oren R, Hsieh CI, Stoy PC, Albertson J, McCarthy HR, Harrell P, Katul GG (2006) Estimating the uncertainty in annual net ecosystem carbon exchange: spatial variation in turbulent fluxes and sampling errors in eddy-covariance measurements. *Global Change Biol* 12:883–896
- Pachsky LB, Hesketh JD, Acock B (1996) An adequate model of photosynthesis I. Parameterization, validation and comparison of models. *Agric Syst* 50:209–225

- Peri PL, Moote DJ, McNeil DL (2005) Modelling photosynthetic efficiency ( $\alpha$ ) for the light-response curve of cocksfoot leaves grown under temperate field conditions. *Eur J Agron* 22:277–292
- Peterson RB (1990) Effects of irradiance on the in vivo  $\text{CO}_2\text{:O}_2$  specificity factor in tobacco using simultaneous gas exchange and fluorescence techniques. *Plant Physiol* 94:892–898
- Phillips OL, and 65 others (2009) Drought sensitivity of the Amazon rainforest. *Science* 323:1344–1347
- Rice AH, Pyle EH, Saleska SR, Hutrya L, Palace M, Keller M, de Camargo PB, Portilho K, Marques DF, Wofsy SC (2004) Carbon balance and vegetation dynamics in an old-growth Amazonian forest. *Ecol Appl* 14(Supplement):S55–S71
- Robinson J (1988) Does  $\text{O}_2$  photoreduction occur within chloroplasts in vivo? *Physiol Plant* 72:666–680
- Saleska SR, Miller SD, Matross DM, Goulden M, Wofsy SC, da Rocha HR, de Camargo PB, Crill P, Daube BC, de Freitas HC, Hutrya L, Keller M, Kirchoff V, Menton M, Munger JW, Pyle EH, Rice AH, Silva H (2003) Carbon in Amazon forests: unexpected seasonal fluxes and disturbance-induced losses. *Science* 302:1554–1557
- Santos Junior UM (2003) *Ecofisiologia de espécies arbóreas plantadas sobre área degradada por atividade petrolífera na Amazônia Central*. INPA/UFAM, Manaus pp 135
- Sharkey TD (1988) Estimating the rate of photorespiration in leaves. *Physiol Plant* 73:666–680
- Sharp RE, Mathews MA, Boyer JS (1984) Kok effect and the quantum yield of photosynthesis: light partially inhibits dark respiration. *Plant Physiol* 75:95–101
- Silva CEM, Gonçalves JFC, Alves EG (2011) Photosynthetic traits and water use species growing on abandoned pasture in different periods of precipitation in Amazonia. *Photosynthetica* 49:246–252
- Singsaas EL, Ort DR, DeLucia EH (2001) Variation in measured values of photosynthetic quantum yield in ecophysiological studies. *Oecologia* 128:15–23
- Stoy PC, Katul GG, Siqueira MBS, Juang J-Y, Novick KA, Uebelherr JM, Oren R (2006) *Agric For Meteorol* 141:2–18
- Sullivan NH, Bolstad PV, Vose JM (1996) Estimates of net photosynthetic parameters for twelve tree species in mature forests of the southern Appalachians. *Tree Physiol* 16:397–406
- Thomas SC, Bazzaz FA (1999) Asymptotic height as predictor of photosynthetic characteristics in Malaysian rain forest trees. *Ecology* 80:1607–1622
- Thornley JHM (1976) *Mathematical models in plant physiology. A quantitative approach to problems in plant and crop physiology*. Academic Press, London
- Thornley JHM (1998) Dynamic model of leaf photosynthesis with acclimation to light and nitrogen. *Ann Bot* 81:421–430
- Tian HQ, Melillo JM, Kicklighter DW, McGuire AD, Helfrich JVK III, Moore BIII, Vörösmarty CJ (1998) Effect of interannual climate variability on carbon storage in Amazonian ecosystems. *Nature* 396:664–667
- Tian HQ, Melillo JM, Kicklighter DW, McGuire AD, Helfrich J III, Moore B III, Vorosmarty CJ (2000) Climatic and biotic controls on annual carbon storage in Amazonian ecosystems. *Glob Ecol Biogeogr* 9:315–335
- Vervuren PJA, Beurskens SMJH, Blom CWPM (1999) Light acclimation,  $\text{CO}_2$  response and long-term capacity of underwater photosynthesis in three terrestrial plant species. *Plant Cell Environ* 22:959–968
- Zhan X, Xue Y, Collatz GJ (2003) An analytical approach for estimating  $\text{CO}_2$  and heat fluxes over the Amazonian region. *Ecol Model* 162:97–117